



CERN-PPE 91/183

29th October, 1991

**A Study of Bose-Einstein Correlations
in e^+e^- Annihilation at 91 GeV**

The ALEPH Collaboration*

Abstract

This paper describes a study of Bose-Einstein correlations made using the ALEPH detector at LEP. The correlations are found to enhance the two particle differential cross section for pairs of identical pions by a factor which can be roughly parametrized by $R(Q) = 1 + \lambda \exp(-Q^2 \sigma^2)$, where Q is the difference in the 3-momenta of the two pions in their centre of mass frame, $\lambda = 0.51 \pm 0.04 \pm 0.11$ and $\sigma = 3.3 \pm 0.2 \pm 0.8 \text{ GeV}^{-1}$, which corresponds to a source size of $0.65 \pm 0.04 \pm 0.16 \text{ fm}$. The large systematic errors on these results reflect their strong dependence on the choice of the reference sample used in the analysis. This problem is believed to occur primarily because of uncertainties in the rates of resonance production and a lack of knowledge about the pion-pion strong interaction. No significant correlations are seen amongst like-charged pion-kaon pairs.

(To be submitted to Zeitschrift für Physik C.)

* See following pages for list of authors.

- D. Decamp, B. Deschizeaux, C. Goy, J.-P. Lees, M.-N. Minard
Laboratoire de Physique des Particules (LAPP), IN²P³-CNRS, 74019 Annecy-le-Vieux Cedex, France
- R. Alemany, J.M. Crespo, M. Delfino, E. Fernandez, V. Gaitan, Ll. Garrido, Ll.M. Mir, A. Pacheco
Laboratorio de Fisica de Altas Energias, Universidad Autonoma de Barcelona, 08193 Bellaterra (Barcelona), Spain⁸
- M.G. Catanesi, D. Creanza, M. de Palma, A. Farilla, G. Iaselli, G. Maggi, M. Maggi, S. Natali, S. Nuzzo, M. Quattromini, A. Ranieri, G. Raso, F. Romano, F. Ruggieri, G. Selvaggi, L. Silvestris, P. Tempesta, G. Zito
INFN Sezione di Bari e Dipartimento di Fisica dell' Universita', 70126 Bari, Italy
- Y. Gao, H. Hu,²¹ D. Huang, X. Huang, J. Lin, J. Lou, C. Qiao,²¹ T. Ruan,²¹ T. Wang, Y. Xie, D. Xu, R. Xu, J. Zhang, W. Zhao
Institute of High-Energy Physics, Academia Sinica, Beijing, The People's Republic of China⁹
- W.B. Atwood,² L.A.T. Bauerdick, F. Bird,⁴ E. Blucher, G. Bonvicini, F. Bossi, J. Boudreau, T.H. Burnett,³ H. Drevermann, R.W. Forty, C. Grab,²³ R. Hagelberg, S. Haywood, J. Hilgart, B. Jost, M. Kasemann,²⁸ J. Knobloch, A. Lacourt, E. Lançon, I. Lehraus, T. Lohse, A. Lusiani, A. Marchioro, M. Martinez, P. Mato, S. Menary,²⁹ T. Meyer, A. Minten, A. Miotto, R. Miquel, H.-G. Moser, J. Nash, P. Palazzi, F. Ranjard, G. Redlinger, L. Rolandi,³⁰ A. Roth,³² J. Rothberg,³ M. Saich, D. Schlatter, M. Schmelling, W. Tejessy, H. Wachsmuth, S. Wasserbaech, W. Wiedenmann, W. Witzeling, J. Wotschack
European Laboratory for Particle Physics (CERN), 1211 Geneva 23, Switzerland
- Z. Ajaltouni, F. Badaud, M. Bardadin-Otwinowska, A.M. Bencheikh, R. El Fellous, A. Falvard, P. Gay, C. Guicheney, P. Henrard, J. Jousset, B. Michel, J-C. Montret, D. Pallin, P. Perret, B. Pietrzyk, J. Proriol, F. Prulhière, G. Stimpff
Laboratoire de Physique Corpusculaire, Université Blaise Pascal, IN²P³-CNRS, Clermont-Ferrand, 63177 Aubière, France
- J.D. Hansen, J.R. Hansen, P.H. Hansen, R. Møllerud, B.S. Nilsson
Niels Bohr Institute, 2100 Copenhagen, Denmark¹⁰
- I. Efthymiopoulos, E. Simopoulou, A. Vayaki
Nuclear Research Center Demokritos (NRCDC), Athens, Greece
- J. Badier, A. Blondel, G. Bonneaud, J.C. Briant, G. Fouque, A. Gamess, J. Harvey, S. Orteu, A. Rosowsky, A. Rougé, M. Rumpf, R. Tanaka, H. Videau
Laboratoire de Physique Nucléaire et des Hautes Energies, Ecole Polytechnique, IN²P³-CNRS, 91128 Palaiseau Cedex, France
- D.J. Candlin, E. Veitch
Department of Physics, University of Edinburgh, Edinburgh EH9 3JZ, United Kingdom¹¹
- L. Moneta, G. Parrini
Dipartimento di Fisica, Università di Firenze, INFN Sezione di Firenze, 50125 Firenze, Italy
- M. Corden, C. Georgiopoulos, M. Ikeda, J. Lannutti, D. Levinthal,¹⁶ M. Mermikides, L. Sawyer
Supercomputer Computations Research Institute and Dept. of Physics, Florida State University, Tallahassee, FL 32306, USA^{13,14,15}
- A. Antonelli, R. Baldini, G. Bencivenni, G. Bologna,⁵ P. Campana, G. Capon, F. Cerutti, V. Chiarella, B. D'Ettore-Piazzoli,³⁴ G. Felici, P. Laurelli, G. Mannocchi,⁶ F. Murtas, G.P. Murtas, L. Passalacqua, M. Pepe-Altarelli, P. Picchi,⁵ P. Zografou
Laboratori Nazionali dell'INFN (LNF-INFN), 00044 Frascati, Italy
- B. Alton, O. Boyle, P. Colrain, A.W. Halley, I. ten Have, J.G. Lynch, W. Maitland, W.T. Morton, C. Raine, J.M. Scarr, K. Smith, A.S. Thompson, R.M. Turnbull
Department of Physics and Astronomy, University of Glasgow, Glasgow G12 8QQ, United Kingdom¹¹

B. Brandl, O. Braun, R. Geiges, C. Geweniger, P. Hanke, V. Hepp, E.E. Kluge, Y. Maumary, A. Putzer, B. Rensch, A. Stahl, K. Tittel, M. Wunsch

Institut für Hochenergiephysik, Universität Heidelberg, 6900 Heidelberg, Fed. Rep. of Germany¹⁷

A.T. Belk, R. Beuselinck, D.M. Binnie, W. Cameron, M. Cattaneo, P.J. Dornan,¹ S. Dugeay, A.M. Greene, J.F. Hassard, N.M. Lieske, S.J. Patton, D.G. Payne, M.J. Phillips, J.K. Sedgbeer, G. Taylor, I.R. Tomalin, A.G. Wright

Department of Physics, Imperial College, London SW7 2BZ, United Kingdom¹¹

P. Girtler, D. Kuhn, G. Rudolph

Institut für Experimentalphysik, Universität Innsbruck, 6020 Innsbruck, Austria¹⁹

C.K. Bowdery, T.J. Brodbeck, A.J. Finch, F. Foster, G. Hughes, D. Jackson, N.R. Keemer, M. Nuttall, A. Patel, T. Sloan, S.W. Snow, E.P. Whelan

Department of Physics, University of Lancaster, Lancaster LA1 4YB, United Kingdom¹¹

T. Barczewski, K. Kleinknecht, J. Raab, B. Renk, S. Roehn, H.-G. Sander, H. Schmidt, F. Steeg, S.M. Walther, B. Wolf

Institut für Physik, Universität Mainz, 6500 Mainz, Fed. Rep. of Germany¹⁷

J.-J. Aubert, C. Benchouk, V. Bernard, A. Bonissent, J. Carr, P. Coyle, J. Drinkard, F. Etienne, S. Papalexiou, P. Payre, Z. Qian, D. Rousseau, P. Schwemling, M. Talby

Centre de Physique des Particules, Faculté des Sciences de Luminy, IN²P³-CNRS, 13288 Marseille, France

S. Adlung, H. Becker, W. Blum, D. Brown, P. Cattaneo,³¹ G. Cowan, B. Dehning, H. Dietl, F. Dydak,²⁶ M. Fernandez-Bosman, T. Hansl-Kozanecka,^{2,22} A. Jahn, W. Kozanecki,² E. Lange, J. Lauber, G. Lütjens, G. Lutz, W. Männer, Y. Pan, R. Richter, H. Rotscheidt, J. Schröder, A.S. Schwarz, R. Settles, U. Stierlin, U. Stiegler, R. St. Denis, M. Takashima, J. Thomas,⁴ G. Wolf

Max-Planck-Institut für Physik und Astrophysik, Werner-Heisenberg-Institut für Physik, 8000 München, Fed. Rep. of Germany¹⁷

V. Bertin, J. Boucrot, O. Callot, X. Chen, A. Cordier, M. Davier, J.-F. Grivaz, Ph. Heusse, P. Janot, D.W. Kim,²⁰ F. Le Diberder, J. Lefrançois,¹ A.-M. Lutz, M.-H. Schune, J.-J. Veillet, I. Videau, Z. Zhang, F. Zomer

Laboratoire de l'Accélérateur Linéaire, Université de Paris-Sud, IN²P³-CNRS, 91405 Orsay Cedex, France

D. Abbaneo, S.R. Amendolia, G. Bagliesi, G. Batignani, L. Bosisio, U. Bottigli, C. Bradaschia, M. Carpinelli, M.A. Ciocci, R. Dell'Orso, I. Ferrante, F. Fidecaro,¹ L. Foà, E. Focardi, F. Forti, C. Gatto, A. Giassi, M.A. Giorgi, F. Ligabue, E.B. Mannelli, P.S. Marrocchesi, A. Messineo, F. Palla, G. Sanguinetti, J. Steinberger, R. Tenchini, G. Tonelli, G. Triggiani, C. Vannini, A. Venturi, P.G. Verdini, J. Walsh

Dipartimento di Fisica dell'Università, INFN Sezione di Pisa, e Scuola Normale Superiore, 56010 Pisa, Italy

J.M. Carter, M.G. Green, P.V. March, T. Medcalf, I.S. Quazi, J.A. Strong, L.R. West, T. Wildish

Department of Physics, Royal Holloway & Bedford New College, University of London, Surrey TW20 OEX, United Kingdom¹¹

D.R. Botterill, R.W. Clift, T.R. Edgecock, M. Edwards, S.M. Fisher, T.J. Jones, P.R. Norton, D.P. Salmon, J.C. Thompson

Particle Physics Dept., Rutherford Appleton Laboratory, Chilton, Didcot, Oxon OX11 0QX, United Kingdom¹¹

B. Bloch-Devaux, P. Colas, E. Locci, S. Loucatos, E. Monnier, P. Perez, J.A. Perlas, F. Perrier, J. Rander, J.-F. Renardy, A. Roussarie, J.-P. Schuller, J. Schwindling, B. Vallage

Département de Physique des Particules Élémentaires, CEN-Saclay, 91191 Gif-sur-Yvette Cedex, France¹⁸

J.G. Ashman, C.N. Booth, C. Buttar, R.E. Carney, S. Cartwright, F. Combley, M. Dogru, F. Hatfield, J. Martin, D. Parker, P. Reeves, L.F. Thompson

*Department of Physics, University of Sheffield, Sheffield S3 7RH, United Kingdom*¹¹

E. Barberio, S. Brandt, C. Grupen, H. Meinhard, L. Mirabito,³³ U. Schäfer, H. Seywerd
*Fachbereich Physik, Universität Siegen, 5900 Siegen, Fed. Rep. of Germany*¹⁷

G. Ganis, G. Giannini, B. Gobbo, F. Ragusa,²⁵
Dipartimento di Fisica, Università di Trieste e INFN Sezione di Trieste, 34127 Trieste, Italy

L. Bellantoni, D. Cinabro, J.S. Conway, D.F. Cowen,²⁴ Z. Feng, D.P.S. Ferguson, Y.S. Gao, J. Grahl, J.L. Harton,
R.C. Jared,⁷ R.P. Johnson,²⁷ B.W. LeClaire, C. Lishka, Y.B. Pan, J.R. Pater, Y. Saadi, V. Sharma, Z.H. Shi,
Y.H. Tang, A.M. Walsh, J.A. Wear,²⁷ F.V. Weber, M.H. Whitney, Sau Lan Wu, G. Zobernig
*Department of Physics, University of Wisconsin, Madison, WI 53706, USA*¹²

(Submitted to Physics Letters B)

¹Now at CERN, PPE Division, 1211 Geneva 23, Switzerland.

²Permanent address: SLAC, Stanford, CA 94309, USA.

³Permanent address: University of Washington, Seattle, WA 98195, USA.

⁴Now at SSCL, Dallas, TX, U.S.A.

⁵Also Istituto di Fisica Generale, Università di Torino, Torino, Italy.

⁶Also Istituto di Cosmo-Geofisica del C.N.R., Torino, Italy.

⁷Permanent address: LBL, Berkeley, CA 94720, USA.

⁸Supported by CAICYT, Spain.

⁹Supported by the National Science Foundation of China.

¹⁰Supported by the Danish Natural Science Research Council.

¹¹Supported by the UK Science and Engineering Research Council.

¹²Supported by the US Department of Energy, contract DE-AC02-76ER00881.

¹³Supported by the US Department of Energy, contract DE-FG05-87ER40319.

¹⁴Supported by the NSF, contract PHY-8451274.

¹⁵Supported by the US Department of Energy, contract DE-FC05-85ER250000.

¹⁶Supported by SLOAN fellowship, contract BR 2703.

¹⁷Supported by the Bundesministerium für Forschung und Technologie, Fed. Rep. of Germany.

¹⁸Supported by the Institut de Recherche Fondamentale du C.E.A.

¹⁹Supported by Fonds zur Förderung der wissenschaftlichen Forschung, Austria.

²⁰Supported by the Korean Science and Engineering Foundation and Ministry of Education.

²¹Supported by the World Laboratory.

²²On leave of absence from MIT, Cambridge, MA 02139, USA.

²³Now at ETH, Zürich, Switzerland.

²⁴Now at California Institute of Technology, Pasadena, CA 91125, USA.

²⁵Now at Dipartimento di Fisica, Università di Milano, Milano, Italy.

²⁶Also at CERN, PPE Division, 1211 Geneva 23, Switzerland.

²⁷Now at University of California, Santa Cruz, CA 95064, USA.

²⁸Now at DESY, Hamburg, Germany.

²⁹Now at Cornell University, Ithaca, NY 14853, USA.

³⁰Also at Dipartimento di Fisica, Università di Trieste, Trieste, Italy.

³¹Now at INFN, Pavia, Italy.

³²Now at Lufthansa, Hamburg, Germany.

³³Now at Institut de Physique Nucléaire de Lyon, 69622 Villeurbanne, France.

³⁴Also at Università di Napoli, Dipartimento di Scienze Fisiche, Napoli, Italy.

1 Introduction

In 1954, it was realised [1] that by studying correlations among fluctuations in the light intensity from a distant star, one could determine the star's angular diameter. Six years later, the size of the particle source in $p\bar{p}$ collisions was measured, by applying the same theory to the correlations seen amongst the like-charged pions produced [2]. The theory has since also been applied to e^+e^- collisions [3,4,5,6,7]. This paper presents a study of these 'Bose-Einstein correlations' made using the ALEPH detector at the LEP e^+e^- collider.

The paper is organised as follows. Section 2 summarises the theory of Bose-Einstein correlations. Section 3 describes the analysis techniques used to study the correlations, and provides details of the event and track selection cuts. Section 4 presents an analysis of the Bose-Einstein effect seen in the data as a function of the single variable Q , which is the difference in the 3-momenta of the two pions in their rest frame. Comparisons with a Monte Carlo simulation are made. Section 5 examines the large systematic effects which were seen in this study. In addition, the effect of long-lived particles on the results is considered, and it is shown that no significant correlations exist among like-charged pion-kaon pairs. A brief description of more detailed studies made of the source shape, is presented in Section 6.

2 Theory

For a pair of identical bosons(fermions), the quantum mechanical wave-function must be symmetric(antisymmetric) under particle exchange. This requirement alters the two-particle differential cross section for the production of identical particles from a source, whose distribution in space-time x is given by $\rho(x)$, by a factor [8,9,10]

$$R(\Delta p) = 1 \pm \lambda |\tilde{\rho}(\Delta p)|^2, \quad (1)$$

where the $+(-)$ sign applies if the spatial wave-function of the particles is symmetric(antisymmetric) under particle exchange. The parameter λ lies in the range zero to one, being zero for a completely coherent source and one for a completely incoherent one. The 4-vector Δp is the difference in the 4-momenta of the two particles and $\tilde{\rho}(\Delta p)$ is the four-dimensional Fourier transform of $\rho(x)$, normalised such that $\tilde{\rho}(\Delta p) \rightarrow 1$ as $\Delta p \rightarrow 0$. i.e.

$$\tilde{\rho}(\Delta p) = \frac{\int_{\text{source}} \rho(x) \exp(i\Delta p \cdot x) d^4x}{\int_{\text{source}} \rho(x) d^4x}. \quad (2)$$

As a pair of identical pions must have a symmetric spatial wave-function, it follows from eqn. (1) that their two-particle differential cross section is enhanced by a factor which tends towards a maximum of $(1 + \lambda)$ for pions of identical 4-momenta.

In deriving eqn. (1), it is assumed that there are no significant correlations between the position at which a particle is produced in the source and its

momentum. Such correlations can arise if the emitters which make up the source are not identical, or if they move with different velocities [11] (unless the energy spectrum of the emitters is flat and extremely wide as assumed in [9]).

If one were to assume that the source could be described by a spherically symmetric Gaussian distribution which decayed exponentially with time

$$\rho(\mathbf{r}, t) \propto \exp(-\mathbf{r}^2/2\sigma^2) \exp(-t/\tau) \quad (3)$$

then for identical pions

$$R(\mathbf{q}, q_0) = 1 + \frac{\lambda \exp(-\mathbf{q}^2 \sigma^2)}{(1 + q_0^2 \tau^2)}. \quad (4)$$

where $\mathbf{q} = \mathbf{p}_1 - \mathbf{p}_2$ and $q_0 = E_1 - E_2$.

However, in the case of $e^+e^- \rightarrow$ hadrons, the source is far more likely to be in the form of a long, thin, rapidly expanding colour string [12] and strong correlations are expected between the positions in the string at which particles are produced and their momenta [13]. It is expected that all particles of any given momentum are emitted from a segment of the string whose r.m.s. length, σ , in the particle rest frame, is independent of that momentum. Two pions with similar 3-momenta will therefore have production points which, measured in their (almost) common rest frame, are separated by a distance of this order. In this rest frame, they will therefore exhibit a Bose-Einstein enhancement appropriate to the length σ and not to the length of the entire string [11,14]. If one makes the additional assumption that the width of each string segment is equal to its length, then the expected Bose-Einstein enhancement will be given by eqn. (4) when measured in the rest frame of each pair ($E_1 = E_2$). That is

$$R(Q) = 1 + \lambda \exp(-Q^2 \sigma^2) \quad (5)$$

where $Q = \sqrt{(\mathbf{p}_1 - \mathbf{p}_2)^2 - (E_1 - E_2)^2}$, which is a Lorentz invariant.

The parametrization of the Bose-Einstein enhancement given in eqn. (5) will be used for the majority of the work presented in this paper. It has the advantage of being a simple function of a single variable, Q , and previous work [3,4,5,6,7] has shown that it fits the data well.

3 Experimental Method

3.1 Measuring $R(Q)$

$R(Q)$ is usually determined by dividing the differential cross section for pairs of like-charged pions by that for the pairs in a 'reference sample', which should be free of Bose-Einstein correlations, but would otherwise have a differential cross section identical to that of the like-charged pairs.

One such reference sample consists of pairs of unlike-charged pions. An approximation to $R(Q)$ is then given by

$$r_{+-}(Q) = \frac{N_{++}(Q)}{N_{+-}(Q)}, \quad (6)$$

where $N_{++}(Q)$ and $N_{+-}(Q)$ are the number of like and unlike-charged pairs as a function of Q .

Another method of obtaining a reference sample uses the technique of event mixing. Pairs of pions are formed by combining a pion from the event under study with a pion from a previous event. The momentum vector of each of these pions is measured with respect to a coordinate system defined by the eigenvectors of the sphericity tensor of the event from which it came. If all events comprised two back to back jets moving parallel to the sphericity axis, then apart from the lack of Bose-Einstein correlations, the differential cross section for these 'event-mixed' pairs would be very similar to that of the like-charged pairs. Multi-jet events will tend to invalidate this reference sample, but their effect can be reduced by using only events with a small sphericity. One also needs to ensure that the detector acceptance is similar for each of the two events being mixed. This is done by requiring the three sphericity tensor eigenvectors in the two events to be aligned to within 6° . $R(Q)$ can then be approximated by

$$r_{mix}(Q) = \frac{N_{++}(Q)}{N_{mix}(Q)} \quad (7)$$

where $N_{mix}(Q)$ is the number of event-mixed pairs as a function of Q .

A third method of obtaining a reference sample begins by dividing each event into two halves separated by the plane perpendicular to its sphericity axis. A pion in one event half is then paired with a pion from the other event half, having first reflected the momentum vector of this second pion through the origin. Multi-jet events must again be rejected using a sphericity cut.

Results obtained using each of the first two methods are presented in this paper. The third method is conceptually very similar to the second and gave almost identical results. Comparison of the results obtained using the different reference samples is essential to estimate systematic effects because, as will be shown in Section 4, the reference samples used are far from perfect.

At small Q , Coulomb repulsion/attraction between like/unlike-charged pions moving away from the source alters the expected two pion cross section in the data by the Gamow factors [10]

$$G_l(\eta) \approx \frac{\eta}{\exp(\eta) - 1} \quad (8)$$

$$G_u(\eta) \approx \frac{\eta}{1 - \exp(-\eta)} \quad (9)$$

where $\eta = 2\pi\alpha m_\pi/Q$, α being the electromagnetic coupling constant and m_π the pion mass. This was corrected for by weighting the entries in all like-charged spectra by a factor $1/G_l(\eta)$ and in all unlike-charged spectra by $1/G_u(\eta)$. For $Q > 0.06$ GeV this altered $r_{+-}(Q)$ and $r_{mix}(Q)$ by less than 10% but for $Q < 0.06$ GeV the correction was large. This correction is only approximate, as all particles are assumed to be pions.

3.2 Event and Track Selection

A detailed description of the ALEPH detector may be found in [15]. The following components were the most important for this analysis. A time-projection chamber (TPC) lying between radii of 31 and 180 cm measures up to 21 three-dimensional points for each track. Its resolution is about 200 μm in $r\phi$ and 1 mm in z . It also provides dE/dx information, with a resolution of up to 4.4%, for particle identification. Inside the TPC is a small drift chamber (ITC) which provides up to eight more hits per track. Outside the TPC is an e/γ calorimeter (ECAL), and beyond this a superconducting solenoid providing a 1.5 T magnetic field. A hadron calorimeter (HCAL) surrounds the solenoid.

Triggers based upon the total energy in the ECAL or evidence of a penetrating track passing through the ITC and into the HCAL were used, and together these were 100% efficient for hadronic events.

Offline selection of the hadronic events employed in this analysis used only tracks which passed within 0.5 cm of the interaction point in the $r\phi$ projection and within 5 cm of it in z . This rejected the majority of particles resulting from long-lived particle decays and gamma conversions. The tracks were also required to have at least eight hits in the TPC to ensure a good momentum measurement. Finally, they were required to have at least three hits in the first five layers of the TPC, which in cases where a single particle was incorrectly reconstructed as two or more separate tracks, virtually eliminated the possibility of more than one of these tracks being accepted.

Events were only accepted if they had at least eight of these tracks and their total energy exceeded 10% of the centre of mass energy. This reduced background from non-hadronic events to negligible levels. Requiring a relatively large multiplicity also reduced the effect of short-range charge correlations of dynamical origin. To ensure that events were well contained in the central detector, it was required that their sphericity axes should make an angle to the beam axis of more than 30° . A total of 153000 events passed these cuts. The mean centre of mass energy was 91.41 GeV.

Except where stated otherwise, these events were only used in the analysis if their sphericity was less than 0.03. Only 62000 events passed this cut. It preferentially selected events comprising two back to back jets, which was necessary for the proper functioning of the event mixing technique, and also ensured that the Bose-Einstein enhancement observed would be that for a single, well defined event topology.

Tracks from these events were only used if they had a momentum below 4.5 GeV/c, thus avoiding the limits of phase space where dynamical correlations are strong. In addition it was required that they had a momentum component perpendicular to the sphericity axis of less than 1.2 GeV/c. This rejected tracks resulting from hard gluons.

The TPC is unlikely to resolve hits which are very close together in both $r\phi$ and z . This region was avoided by rejecting pairs of tracks in which the two tracks

passed within 3 cm of each other in $r\phi$ and within 5 cm in z , in any layer of the TPC. Applied alone, this cut would introduce a bias, as the magnetic field in the central detector usually results in two tracks with similar 3-momenta being further apart in space if they are unlike-charged, than if they are like-charged. This bias was removed by also applying the same cut to the separation which the two tracks would have had, if one of them had been produced with the opposite charge to that which it had in reality.

A similar problem affects the dE/dx signals from the TPC, with unlike-charged tracks of similar 3-momenta having on average more dE/dx information than like-charged tracks. Applying tight cuts to the dE/dx to enhance the pion purity would therefore have led to large systematic effects. The dE/dx was, however, used to help reject electrons from gamma conversions and Dalitz pairs. Pairs of tracks in which both tracks had a measured dE/dx which was within three standard deviations of that expected for an electron and more than four standard deviations away from that expected for a pion were rejected. This cut rejected very few non- e^+e^- pairs and hence led to a negligible systematic error. Electrons were also eliminated by rejecting any track with a momentum exceeding 1.5 GeV/c and a signal in the ECAL consistent with that of an electron [16].

4 Analysis of the Data

Figure 1 shows the numbers of like and unlike-charged pairs found in the ALEPH data as a function of Q . Figures 2a,b show $r_{+-}^{data}(Q)$ and $r_{mix}^{data}(Q)$ respectively. Both show clear enhancements in the region $Q < 0.3$ GeV. These can be compared with the corresponding plots of $r_{+-}^{MC}(Q)$ and $r_{mix}^{MC}(Q)$ given in Figures 3a,b respectively, which were obtained from a set of Monte Carlo events in which the Bose-Einstein effect was not simulated.

The Monte Carlo events were generated using DYMU [17] to simulate the reaction $e^+e^- \rightarrow Z^0 \rightarrow q\bar{q}$ including initial and final state radiation, and JETSET 6.3 (parton shower) [12] to simulate the parton cascade and fragmentation. They included a detailed simulation of detector effects and were tuned to reproduce the gross features seen in the ALEPH data. There was a total of 185000 Monte Carlo events with a mean centre of mass energy of 91.16 GeV.

Both $r_{+-}^{MC}(Q)$ and $r_{mix}^{MC}(Q)$ deviate from unity, which indicates that neither of the reference samples used is perfect. Figure 3a shows that $r_{+-}^{MC}(Q)$ falls slowly with decreasing Q . This is caused by long-range charge correlations: pairs at small Q are formed predominantly by pairing particles from the same jet, and assuming that the total charge of a jet is always approximately zero, it is easy to see that there are fewer like-charged combinations available within a jet than unlike-charged ones. $r_{+-}^{MC}(Q)$ also shows small dips near $Q = 0.412$ GeV and $Q = 0.717$ GeV. These are caused by $\pi^+\pi^-$ pairs resulting from the decays $K^0 \rightarrow \pi^+\pi^-$ and $\rho^0 \rightarrow \pi^+\pi^-$, respectively. Figure 3b shows that $r_{mix}^{MC}(Q)$ has a sizeable rise at small Q and a more gentle rise towards large Q . There are three major causes of the rise at small Q : (i) The like-charged pion pairs produced in the decay chain $\eta' \rightarrow \eta\pi^+\pi^-$ followed by $\eta \rightarrow \pi^+\pi^-\pi^0$ are always produced at small Q

[18]. (ii) The event mixing method ignores correlations caused by gluon jets. Although this problem is reduced using the sphericity cut (see Section 3.2), it is not eliminated. (iii) The method overlooks correlations arising from the fact that events initiated by $b\bar{b}$ production tend to be broader than those initiated by light $q\bar{q}$ production. The latter two problems are more serious at LEP than they were at PEP or PETRA because of the more visible jet structure at LEP and the higher proportion of $b\bar{b}$ events.

To the extent that the failings of the reference samples are correctly simulated by the Monte Carlo, one can overcome them by dividing the data by the Monte Carlo: i.e. studying the double ratios:

$$R_{+-}(Q) = r_{+-}^{data}(Q)/r_{+-}^{MC}(Q) = \frac{N_{++}^{data}(Q)}{N_{+-}^{data}(Q)} \bigg/ \frac{N_{++}^{MC}(Q)}{N_{+-}^{MC}(Q)} \quad (10)$$

and

$$R_{mix}(Q) = r_{mix}^{data}(Q)/r_{mix}^{MC}(Q) = \frac{N_{++}^{data}(Q)}{N_{mix}^{data}(Q)} \bigg/ \frac{N_{++}^{MC}(Q)}{N_{mix}^{MC}(Q)}. \quad (11)$$

$R_{+-}(Q)$ and $R_{mix}(Q)$ are plotted in Figures 4a,b respectively. As expected, both are approximately unity outside the region affected by the Bose-Einstein enhancement. $R_{+-}(Q)$ does however show a slight enhancement near $Q = 0.717$ GeV which implies that the Monte Carlo is probably overproducing ρ^0 's. (It produces 1.5 per event).

$R_{+-}(Q)$ and $R_{mix}(Q)$ were fitted in the range $0 < Q < 2$ GeV with the function

$$R_{+-}(Q), R_{mix}(Q) = \kappa(1 + \epsilon Q) [1 + \lambda \exp(-Q^2 \sigma^2)], \quad (12)$$

which is eqn. (5) multiplied by a linear function in Q to try to take account of imperfections in the Monte Carlo simulation. When fitting $R_{+-}(Q)$, the regions $0.388 < Q < 0.436$ GeV and $0.502 < Q < 0.932$ GeV were excluded to remove sensitivity to the production rates of K^0 's and ρ^0 's. The results of the fits have been superimposed over Figures 4a,b and are presented in rows (a) and (b) of Table 1. In this table, the quantity $C_{\lambda\sigma}$ is the correlation coefficient between λ and σ .

The results of the two fits are statistically inconsistent. This problem is discussed in Section 5.

Monte Carlo studies indicate that the fraction of pairs which are identical pions can be well parametrized in the region $0 < Q < 2$ GeV, by the function

$$p(Q) = 0.755 \times (1 - 0.023Q) [1 + 0.13 \exp(-11.6Q)]. \quad (13)$$

Pairs comprising two different particles will not exhibit Bose-Einstein correlations and so will reduce the size of the enhancement seen. One can correct for this by fitting the ratios in Figures 4a,b with a slightly modified version of eqn. (12), namely

$$R_{+-}(Q), R_{mix}(Q) = \kappa(1 + \epsilon Q) [1 + \lambda p(Q) \exp(-Q^2 \sigma^2)]. \quad (14)$$

This yields the results given in rows (c) and (d) of Table 1. In row (e) of this table, these two results have been combined using a simple average. The systematic error on this combined result is taken to be one half of the difference between the two separate results, and is the second of the two errors given for each parameter.

Using the fitted values of λ and σ given in rows (c) and (d), the individual entries in Figures 4a,b can be corrected for the finite pion purity by multiplying each one by a factor

$$\frac{1 + \lambda \exp(-Q^2 \sigma^2)}{1 + p(Q) \lambda \exp(-Q^2 \sigma^2)}. \quad (15)$$

This transforms Figures 4a,b into Figures 5a,b respectively. The curve superimposed over each of Figures 5a,b is eqn. (12), evaluated using the parameters in rows (c) and (d) of Table 1 respectively.

Table 2 compares these results with those obtained from previous experiments. No significant change in the source size with increasing centre of mass energy is visible. However, the large systematic uncertainties greatly limit sensitivity to any such effect. A detailed examination of these systematic effects is presented in the next section.

5 Discussion of Results and Systematics

5.1 Comparison of Monte Carlo and Data

The fits made to the distributions $R_{+-}(Q)$ and $R_{mix}(Q)$ (as defined in eqns. (10) and (11)) would have yielded identical results if $N_{+-}^{data}(Q)/N_{+-}^{MC}(Q)$ and $N_{mix}^{data}(Q)/N_{mix}^{MC}(Q)$ had had the same shape. These two ratios are plotted in Figures 6a,b respectively. $N_{+-}^{data}(Q)/N_{+-}^{MC}(Q)$ rises above unity by about 10% in the region $0.3 < Q < 0.6$ GeV, whereas $N_{mix}^{data}(Q)/N_{mix}^{MC}(Q)$ is reasonably flat with the exception of a small dip at very low Q . It follows that it is primarily an inadequate Monte Carlo simulation of the $\pi^+\pi^-$ spectrum which leads to the inconsistent results given in Section 4. A similar effect has been seen by the TPC-PEP4 collaboration at a centre of mass energy of 29 GeV [19].

The two most likely reasons for the inadequate Monte Carlo simulation of the $\pi^+\pi^-$ spectrum are:

i) It does not simulate final state interactions between particles moving away from the source. The strong interaction between unlike-charged pions is expected to be sizeable and attractive [20] although exact predictions remain elusive. It is therefore quite possible that it accounts for the rise in Figure 6a in the region $0.3 < Q < 0.6$ GeV, but more doubtful that it can explain the drop which occurs in the region $Q < 0.3$ GeV.

ii) The decay chain $\eta' \rightarrow \eta\pi^+\pi^-$ followed by $\eta \rightarrow \pi^+\pi^-\pi^0$ yields many $\pi^+\pi^-$ pairs in the region $Q < 0.3$ GeV [18]. Furthermore there are theoretical arguments which indicate that JETSET may be producing far too many η' 's [21]. (It produces 0.7 η' 's per event and assumes that the rates of η and η' production from the string are equal). If in the Monte Carlo, one ignores pairs in which both tracks

are descendents of the same η' , then the drop seen in the region $Q < 0.3$ GeV of Figure 6a is virtually eliminated (shown by the square points in the figure).

Other possibilities exist, but are unlikely to account for the entire discrepancy. Doubling the production rates of ω^0 's and K^{*0} 's in the Monte Carlo, from their present rates of 1.3 and 1.1 per event respectively, will by itself remove most of the discrepancy. It seems unlikely, however, that such large changes are justified. A further possibility is that the simulation of the kinematics of heavy particle decays (e.g. B hadrons) is inaccurate. However, as only 22% of events contain B hadrons, this too is unlikely to play a major role. The fragmentation process is known to lead to short-range correlations and it is possible that JETSET incorrectly simulates these. However, a similar discrepancy in the $\pi^+\pi^-$ spectrum is also seen when using the HERWIG [22] Monte Carlo, which uses a different fragmentation scheme. Finally, the problem can not arise through an inadequate simulation of multi-jet events, as the Monte Carlo is found to describe the production rates and topology of such events well [23]. Further, if an order α_s^2 matrix elements QCD calculation is used within JETSET, almost identical results are obtained. In addition, the discrepancy does not get worse if the event sphericity cut is removed.

In conclusion, the defects in the Monte Carlo simulation of the $\pi^+\pi^-$ spectrum probably arise because it does not simulate final state strong interactions and it overproduces η' . However, other effects may also be contributing.

This discussion does not necessarily imply that the results obtained using the event mixed reference sample are reliable. This will only be true if the like-charged spectrum is also well simulated by the Monte Carlo (apart from the absence of the Bose-Einstein effect). This is probably not the case, because the like-charged spectrum will also be affected by final state strong interactions and η' decays. (η' decays not only produce many unlike-charged pairs at low Q , but also some like-charged pairs). It therefore remains unclear which reference sample it is best to use.

5.2 Detector Effects

The finite detector resolution could in principle lead to systematic effects by broadening the observed Bose-Einstein enhancement. The Monte Carlo shows, however, that the resolution in Q can be parametrized by $(3.7 + 3.5Q) \times 10^{-3}$ GeV, which is so good that its effect can be ignored.

Low momentum particles can spiral many times inside the TPC and may thus occasionally be reconstructed as several separate tracks, so leading to spurious correlations at low Q . Using the Monte Carlo, however, it was established that the cuts described in Section 3.2 eliminate this problem.

5.3 Residual Bose-Einstein Correlations in the Reference Samples

The three reference samples described in Section 3.1 are not entirely free of the effect of Bose-Einstein correlations. The reason for this is that these correlations tend to bring the π^+ 's in a jet slightly closer together in momentum space than

they would otherwise have been. The same will be true for the π^- 's. Hence, Bose-Einstein correlations *make the jets narrower* and hence increase the probability of unlike-charged or event-mixed pairs of tracks being found close together in momentum space. Calculations similar to those employed in [24] showed that this effect would reduce the size of the observed Bose-Einstein enhancement by only a few percent. Furthermore, this reduction will be largely cancelled out by a similar effect bringing the like-charged pions closer together than would be naively expected. The results given in this paper were therefore not corrected for this effect.

5.4 The Effect of Long-Lived Particles

If two pions have production points which are separated by more than about 10 fm, they will only exhibit a significant Bose-Einstein enhancement if they have extremely small Q (< 0.02 GeV). As there is almost no data in this region, such pairs make virtually no contribution to the observed enhancement. The JETSET Monte Carlo indicates that after applying the cuts of Section 3.2, 27% of like-charged pion pairs in the region $Q < 0.2$ GeV (where the Bose-Einstein enhancement is large) involve the descendent of a weakly decaying particle (excluding cases where both pions are descendents of the *same* weakly decaying particle) and hence will not contribute noticeably to the enhancement. Pion pairs in which one pion results from the decay of a resonance, with a width of less than about 0.02 GeV (e.g. η , ω or ϕ), and the other pion comes from elsewhere, will likewise make no visible contribution to the observed enhancement. JETSET indicates that in the region $Q < 0.2$ GeV, a further 49% of all like-charged pion pairs passing the cuts of Section 3.2, lie in this category. The value of λ seen in the data should thus be no greater than 0.24 ($= 1 - 0.27 - 0.49$), even in the case of a completely incoherent source. Overproduction of η 's in the Monte Carlo may explain why the measured value of λ ($= 0.51 \pm 0.04 \pm 0.11$) is so much larger. If as suggested in [21], one replaces the pions coming (directly or indirectly) from η 's by pions coming from the string, then the percentage of pion pairs which can contribute to the enhancement rises to 40%, which is consistent with the data.

5.5 πK (and πp) Correlations

A check on systematic effects was made by searching for correlations amongst like-charged πK (and πp) pairs, where no effect should be seen. The sample of πK and πp pairs was selected by repeating the event and track selection of Section 3.2, but with the additional requirement that the dE/dx measurements for the two tracks in a pair should be such that, at the three standard deviation level, one track is consistent with being a pion and the other inconsistent. To try to avoid the systematic effects referred to in Section 3.2, the dE/dx measurements of the unlike-charged and event-mixed pairs were smeared to make them as bad as those for the like-charged pairs.

The Monte Carlo indicated that the residual contamination from identical bosons in the sample of like-charged pairs selected above, was only 3% (with a slight Q dependence). Figure 7 shows $R_{+-}(Q)$ as determined from this reference

sample. No significant correlations are visible. To maximise the similarity with the analysis of Section 4, Q was calculated treating both particles as pions. The parameter η in the Gamow correction factors (eqns. (8) and (9)) needed modification however, to take into account that the particles had different mass.

6 More detailed studies of the source shape

This section describes more detailed studies which were made of the source shape. The systematic errors on these results are once again large (approximately $\pm 20\%$) and in view of this, only a brief resumé of them will be given here.

i) Removing the cuts on the event sphericity and on the momentum component of tracks perpendicular to the sphericity axis (see Section 3.2), had negligible effect on the results given in Table 1. This implies that the size of the source does not depend significantly on the event topology.

ii) The results did not display a significant dependence on either the Lorentz boost of the pair relative to the laboratory frame, or on the charged multiplicity of the event.

iii) In the pair rest frame, no significant difference was seen between the dimensions of the source parallel and perpendicular to the sphericity axis.

iv) Equation (4), which assumes that the source is spherical in the laboratory frame, did not fit the data well. The parameter τ^2 tended towards physically meaningless negative values.

v) The enhancement was studied in two-dimensional plots of q^2 versus q_0^2 (notation as in eqn. (4)) and q_t^2 versus q_l^2 (where q_t is the difference in the momentum components of the two pions perpendicular to the sphericity axis in the laboratory frame and $q_l^2 = Q^2 - q_t^2$). Both plots were well described by eqn. (5).

vi) Using the string model, Bowler predicts a Bose-Einstein enhancement [8] of

$$R(q_l^2, q_t^2) \approx 1 + \frac{(A/2)}{(\beta_l^2 q_l^2)^2 - 1} \log(\beta_l^2 |q_l^2|) \exp(-\beta_t^2 q_t^2). \quad (16)$$

In the region $q_l^2 > 0$, this equation fits the data well, with the parameters A and β_l lying within the ranges required for the string model to be compatible with the observed single particle spectra [8]. In the region $q_l^2 < 0$, the observed enhancement was much larger than that predicted by this model (probably because of incorrect assumptions made in the model about the width of the string [5,8]).

7 Conclusions

A study has been made of Bose-Einstein correlations in ALEPH. The Bose-Einstein enhancement can be well parametrized by the formula $R(Q) = 1 + \lambda \exp(-Q^2 \sigma^2)$, where $\lambda = 0.51 \pm 0.04 \pm 0.11$ and $\sigma = 3.3 \pm 0.2 \pm 0.8 \text{ GeV}^{-1}$. This form would be expected if, seen from the rest frame of particles of any given momentum, the source were spherically symmetric with an r.m.s. radius of $\sigma = 0.65 \pm 0.04 \pm 0.16 \text{ fm}$.

This result is comparable with those obtained at lower energy e^+e^- colliders [3,4,5,6]. The value of λ is however somewhat smaller than that recently obtained by the OPAL collaboration [7].

The large systematic errors appear to arise primarily from a lack of knowledge about the $\pi\pi$ strong interaction and because of uncertainties in the rates of resonance production (in particular for η' and η , but also for ω^0 and K^{*0}). These effects lead to an inadequate Monte Carlo simulation of the $\pi^+\pi^-$ spectrum in Q . Reliable measurements of the η' and η production rates are essential if further progress is to be made in this field.

No significant correlations are seen amongst like-charged πK and πp pairs.

Note Added in Proof

After completion of this analysis, we received a preprint from Bowler [25] which states that the Gamow factor greatly overestimates the size of the final state Coulomb interaction. To provide an upper limit on the size of this effect, the analysis was repeated without using the Gamow correction factors. This reduced the value of λ by 15% when using the unlike reference sample and 8% when using the event-mixed reference sample. It had negligible effect on σ .

Acknowledgements

We are indebted to our colleagues in the SL division for the excellent performance of the LEP storage ring. We thank also the engineers and technicians of all our institutions for their support in constructing ALEPH. Those of us from non-member countries thank CERN for its hospitality. We acknowledge helpful comments from M.G. Bowler, B. Lörstad, R. Peschanski and T. Sjöstrand, and thank C. Baugh for his contribution to our analysis.

References

- [1] R. Hanbury-Brown, R.Q. Twiss, *Phil. Mag.* **45** (1954) 663
R. Hanbury-Brown, R.Q. Twiss, *Nature* **178** (1956) 1046
- [2] G. Goldhaber *et al.*, *Phys. Rev.* **120** (1960) 300
- [3] TPC-PEP4 Collaboration, H. Aihara *et al.*, *Phys. Rev.* **D31** (1985) 996
- [4] CLEO Collaboration, P. Avery *et al.*, *Phys. Rev.* **D32** (1985) 2294
- [5] TASSO Collaboration, M. Althoff *et al.*, *Z. Phys.* **C30** (1986) 355
- [6] Mark II Collaboration, I. Juričić *et al.*, *Phys. Rev.* **D39** (1989) 1
- [7] OPAL Collaboration, P.D. Acton *et al.*, CERN-PPE 91-110 (1991)
- [8] M.G. Bowler, *Z. Phys.* **C29** (1985) 617

- [9] G.I. Kopylov, M.I. Podgoretskiĭ, Sov. J. Nucl. Phys. **18** (1974) 336 and **19** (1974) 215
- [10] R. Lednicky, V.L. Lyuboshits, Sov. J. Nucl. Phys. **35** (1982) 770
- [11] W. Hofmann, LBL-23108 (1987)
- [12] T. Sjöstrand and M. Bengtsson, Comp. Phys. Com. **43** (1987) 367
- [13] X. Artru, A. Mennessier, Nucl. Phys. **B70** (1974) 93
- [14] Section 4 of [7]
- [15] ALEPH Collaboration, D. Decamp *et al*, Nucl. Instr. Meth. **A294** (1990) 121.
- [16] The ECAL cuts used are given in: ALEPH Collaboration, D. Decamp *et al*, Phys. Lett. **B244** (1990) 551, equation 6
- [17] J.E. Campagne, Ph.D Thesis, Paris, LPNHEP 89-02
J.E. Campagne and R. Zitoun, Z. Phys. **C43** (1989) 469
- [18] K. Kulka and B. Lörstad, Nucl. Instr. Meth. **A295** (1990) 443
- [19] R.E. Avery, Ph.D. Thesis, LBL-26593 (1989), Figures 5.7 and 5.8
- [20] M.G. Bowler, Z. Phys. **C39** (1988) 81
- [21] M.G. Bowler, Phys. Lett. **B180** (1986) 299
- [22] G. Marchesini, B. Webber, Cavendish-HEP-88/7 (1988) and Nucl. Phys. **B310** (1988) 461
- [23] ALEPH Collaboration, *Properties of Hadronic Z decays and Test of QCD Generators*, to be published
- [24] I. Juričić, Ph.D. Thesis, LBL-24493 (1987), Appendix A
- [25] M.G. Bowler, OUNP-91-23 (1991)

Table 1: Fits to the data as a function of Q using eqns. (12) or (14).

	λ	σ (GeV $^{-1}$)	$C_{\lambda\sigma}$	κ	ϵ (GeV $^{-1}$)	χ^2/NDF	Type of Fit
(a)	0.48 ± 0.03	4.1 ± 0.2	0.39	0.97 ± 0.01	0.02 ± 0.01	77/70	Like/Unlike
(b)	0.30 ± 0.01	2.6 ± 0.1	0.17	0.94 ± 0.01	0.04 ± 0.01	92/95	Like/Mixed
(c)	0.62 ± 0.04	4.1 ± 0.2	0.36	0.97 ± 0.01	0.02 ± 0.01	79/70	As (a) but pure pions
(d)	0.40 ± 0.02	2.5 ± 0.1	0.13	0.93 ± 0.01	0.04 ± 0.01	89/95	As (b) but pure pions
(e)	$0.51 \pm 0.04 \pm 0.11$	$3.3 \pm 0.2 \pm 0.8$	0.31				(c) and (d) combined

Table 2: Fits to Q : Comparison with previous experiments.

Experiment	\sqrt{s} (GeV)	Reference Sample	λ	σ (fm)
ALEPH	91.4	event mixing	0.40 ± 0.02	0.50 ± 0.02
OPAL[7]	91.3	unlike-charged	1.08 ± 0.05	0.93 ± 0.02
TPC-PEP4 [3]	29	event mixing	$0.61 \pm 0.05 \pm 0.06$	$0.65 \pm 0.04 \pm 0.05$
Mark II [6]	29	cluster mixing	$0.45 \pm 0.03 \pm 0.04$	$1.01 \pm 0.09 \pm 0.06$
ALEPH	91.4	unlike-charged	0.62 ± 0.04	0.80 ± 0.04
Mark II [6]	29	unlike-charged	$0.50 \pm 0.03 \pm 0.04$	$0.84 \pm 0.06 \pm 0.05$
TASSO [5]	34.4	unlike-charged	$0.35 \pm 0.03 \pm 0.04^\dagger$	0.80 ± 0.06

† The TASSO result was not corrected for the presence of non-pions. Their value of λ should therefore be compared with that in rows (a) and (b) of Table 1.

Figure Captions

Figure 1: Numbers of like and unlike-charged pairs found in the data, as a function of Q .

Figures 2a,b: $r_{+-}^{data}(Q)$ and $r_{mix}^{data}(Q)$ respectively, for the data.

Figures 3a,b: $r_{+-}^{MC}(Q)$ and $r_{mix}^{MC}(Q)$ respectively, for the Monte Carlo.

Figures 4a,b: $R_{+-}(Q) = r_{+-}^{data}(Q)/r_{+-}^{MC}$ and $R_{mix}(Q) = r_{mix}^{data}/r_{mix}^{MC}$ respectively.

Figures 5a,b: Same as Figures 4a,b respectively, but corrected for non-pion background.

Figure 6a: The triangular points show the ratio of the numbers of unlike-charged pairs found in the data to the numbers found in the Monte Carlo: as a function of Q . The square points show this ratio after elimination of all pairs in which both tracks are descendents of the same η' .

Figure 6b: The ratio of the numbers of event-mixed pairs found in the data to the numbers found in the Monte Carlo, as a function of Q .

Figure 7: $R_{+-}(Q)$ for $\pi^\pm K^\pm$ pairs

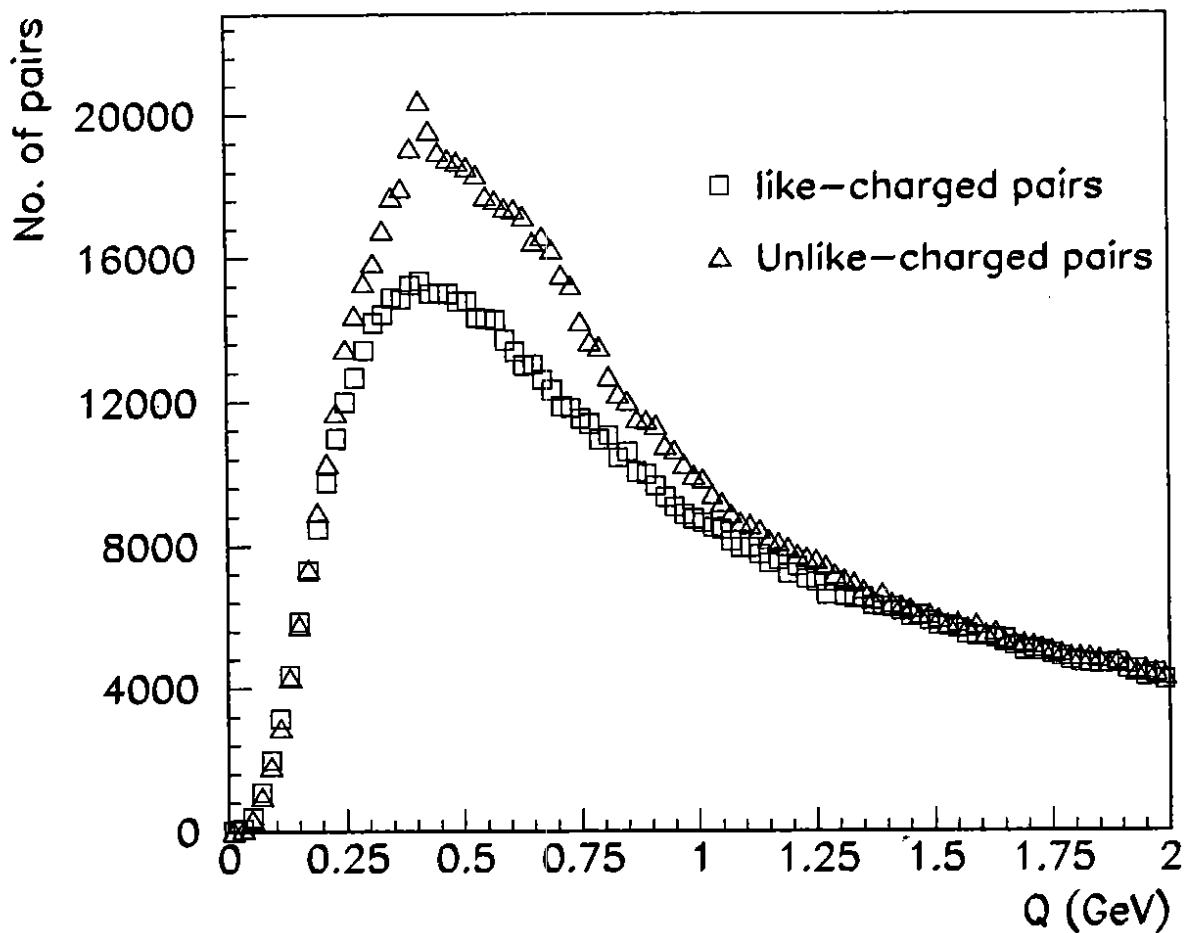


Figure 1 : No. of pairs in data

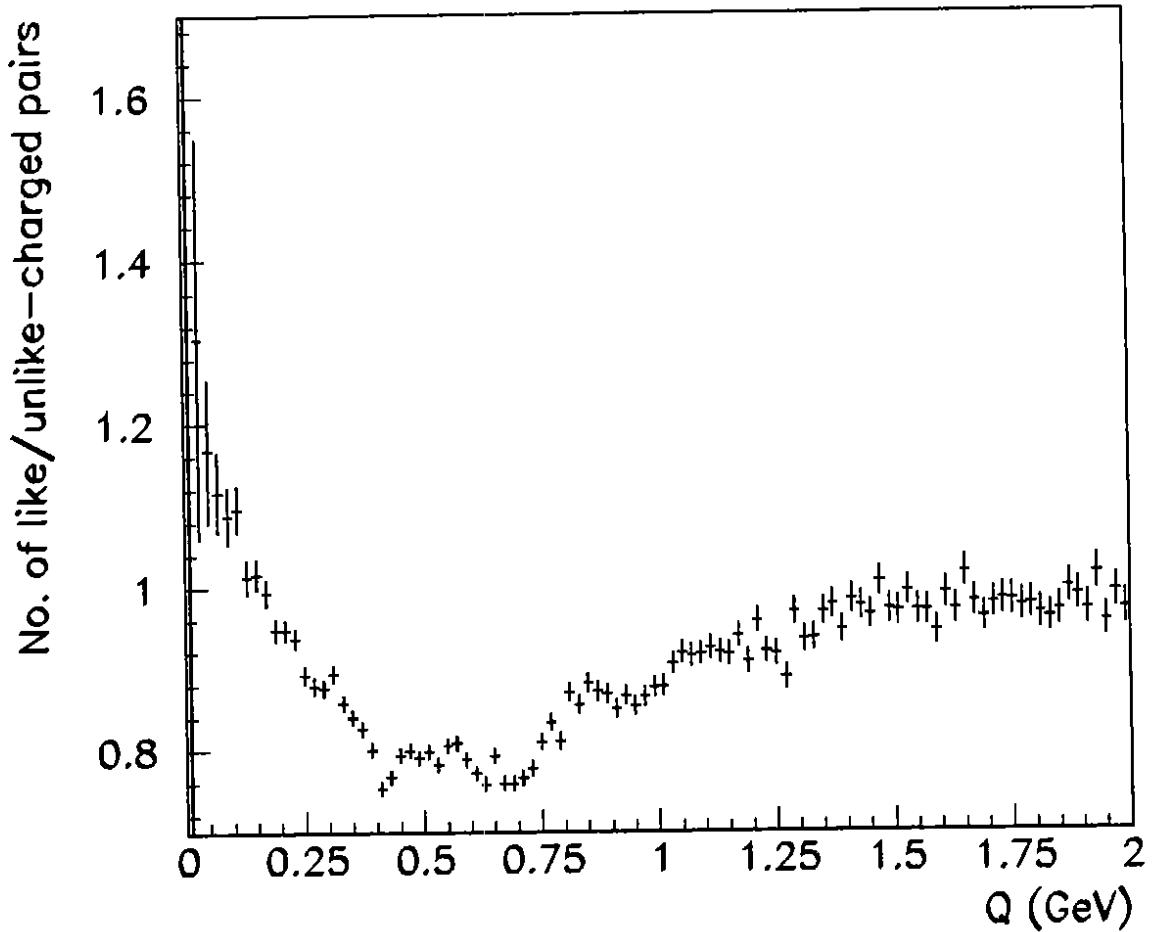


Figure 2a : $r_{+-}^{\text{data}}(Q) = N_{++}^{\text{data}}(Q) / N_{+-}^{\text{data}}(Q)$

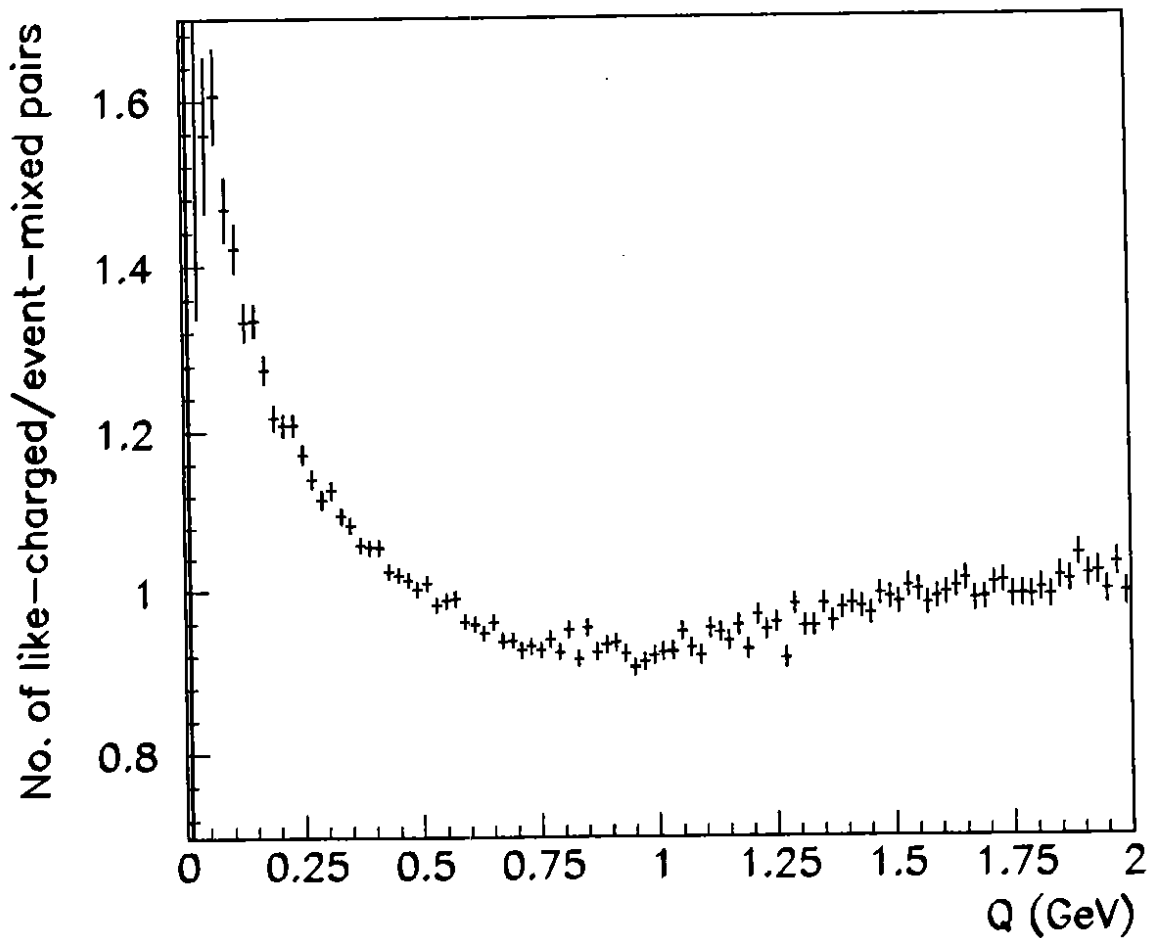


Figure 2b : $r_{\text{mix}}^{\text{data}}(Q) = N_{++}^{\text{data}}(Q) / N_{\text{mix}}^{\text{data}}(Q)$

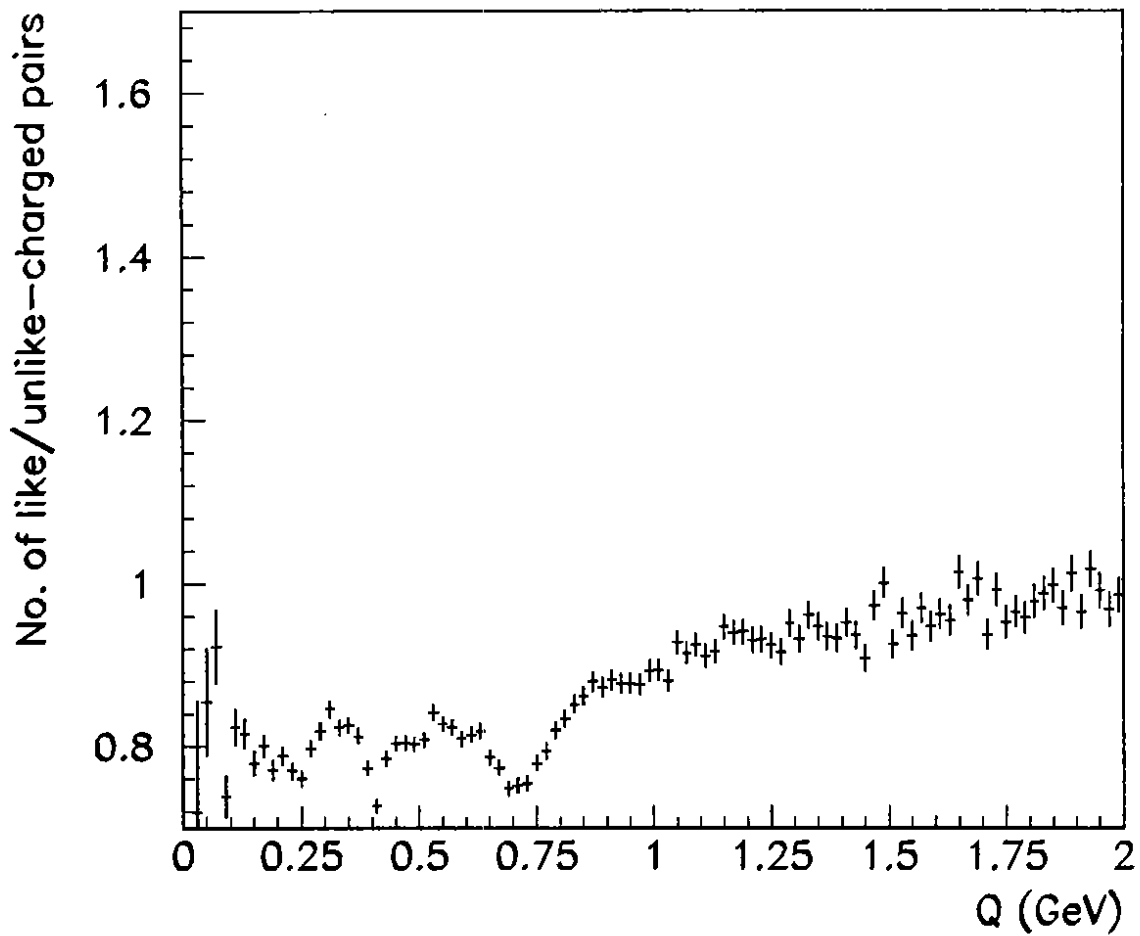


Figure 3a : $r_{+-}^{MC}(Q) = N_{+-}^{MC}(Q) / N_{-+}^{MC}(Q)$

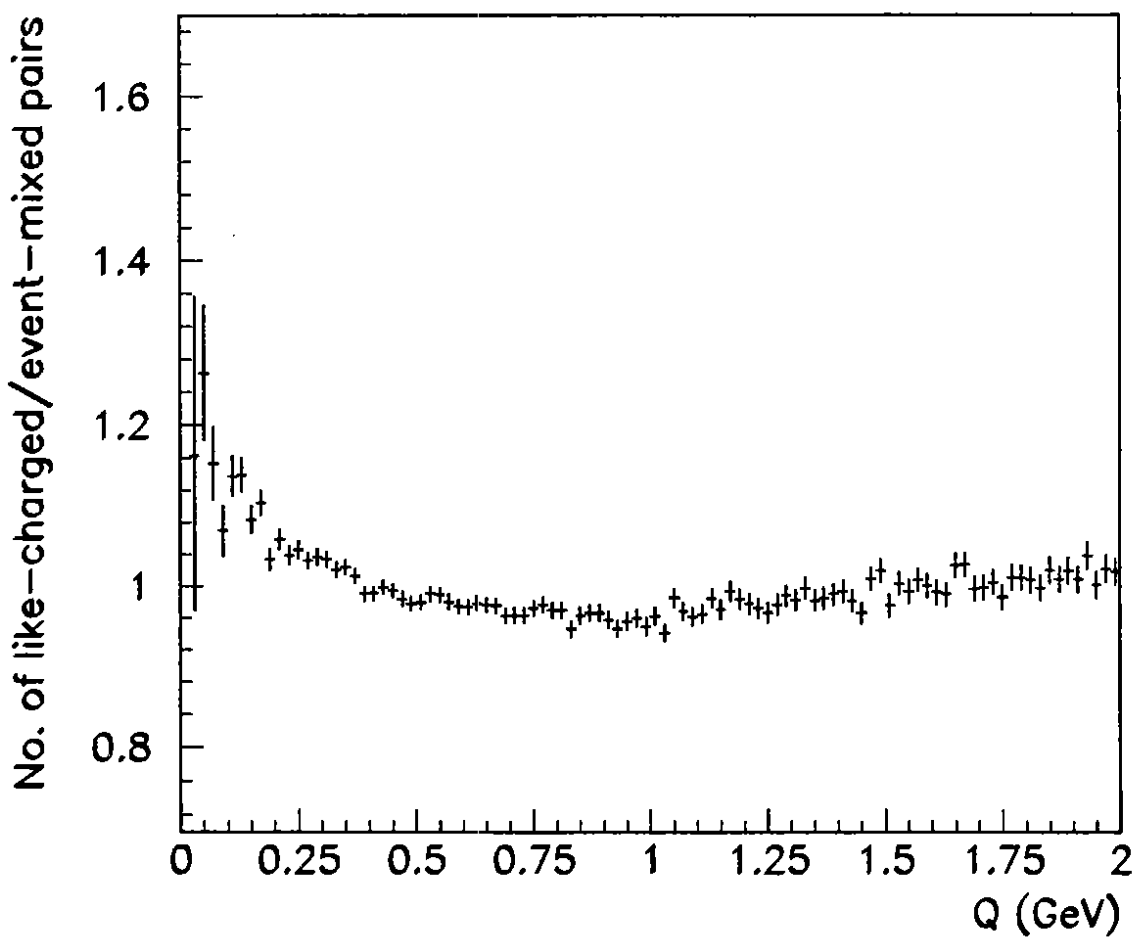


Figure 3b : $r_{mix}^{MC}(Q) = N_{++}^{MC}(Q) / N_{mix}^{MC}(Q)$

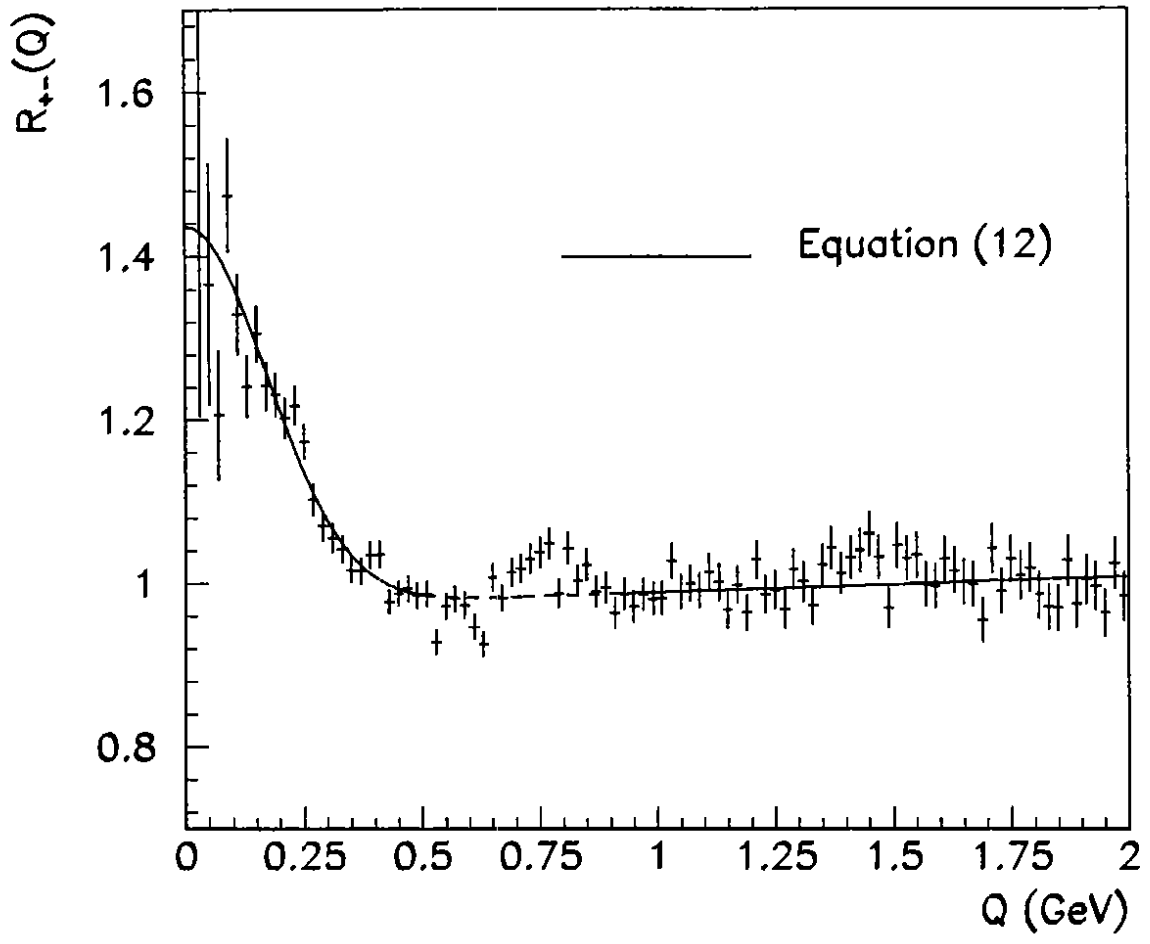


Figure 4a : $R_{+-}(Q) = r_{+-}^{\text{data}}(Q) / r_{+-}^{\text{MC}}(Q)$

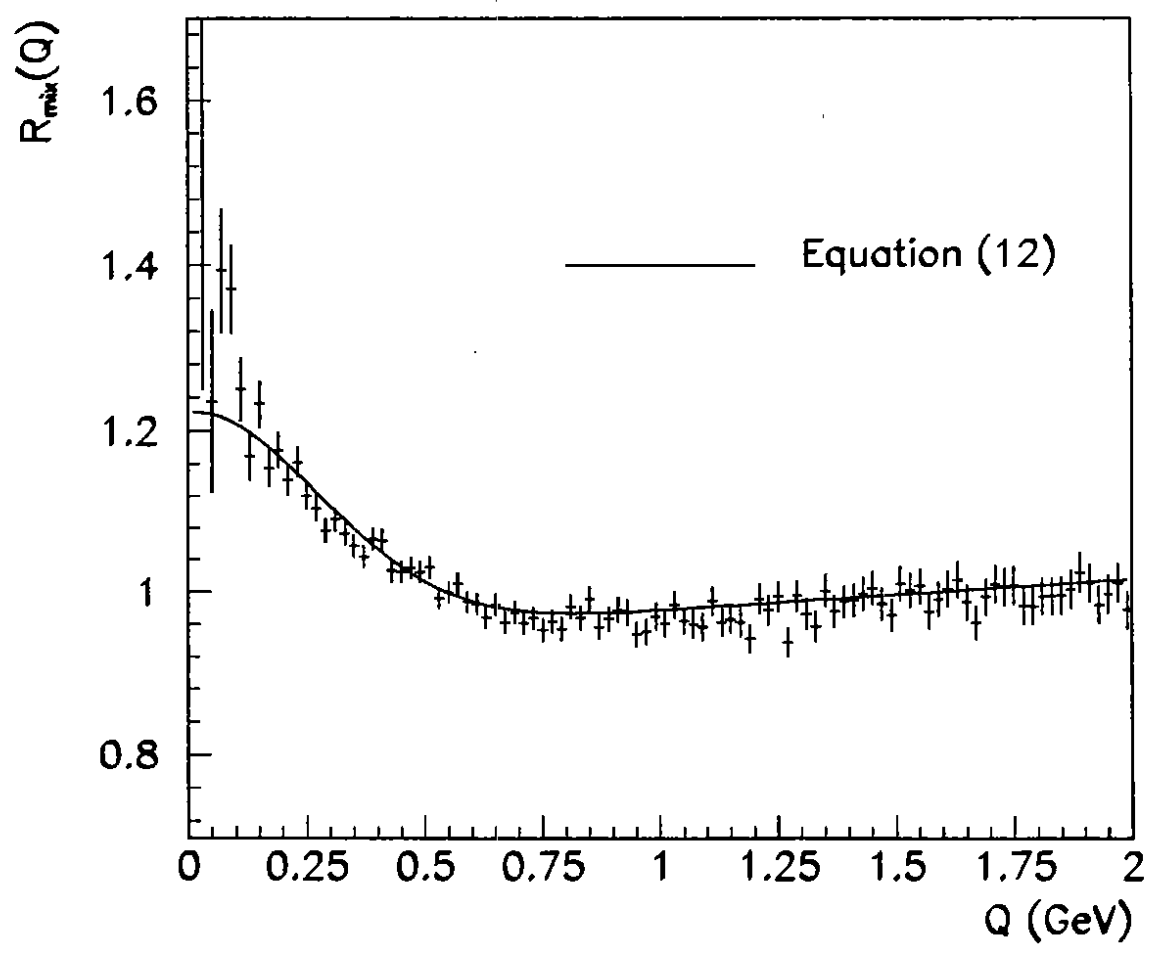


Figure 4b : $R_{\text{mix}}(Q) = r_{\text{mix}}^{\text{data}}(Q) / r_{\text{mix}}^{\text{MC}}(Q)$

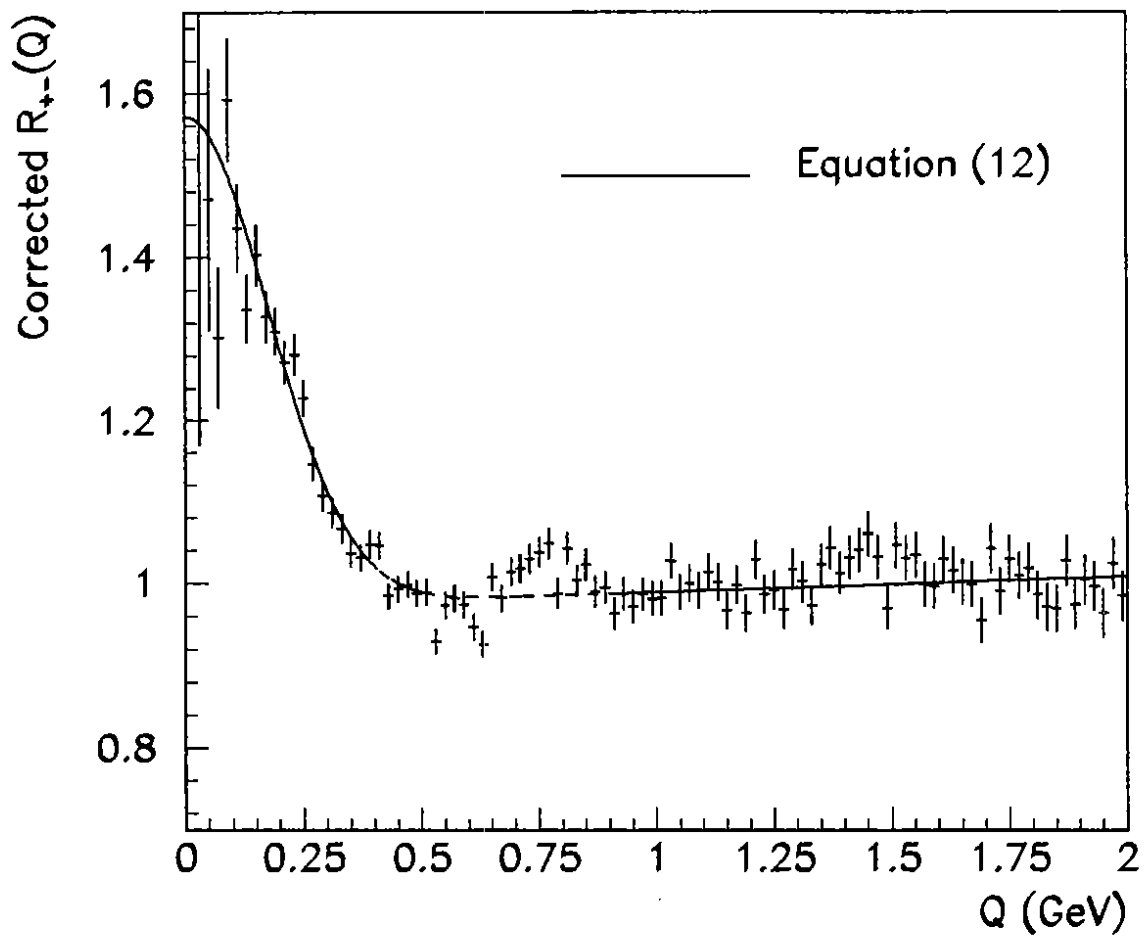


Figure 5a : Corrected $R_{+-}(Q)$

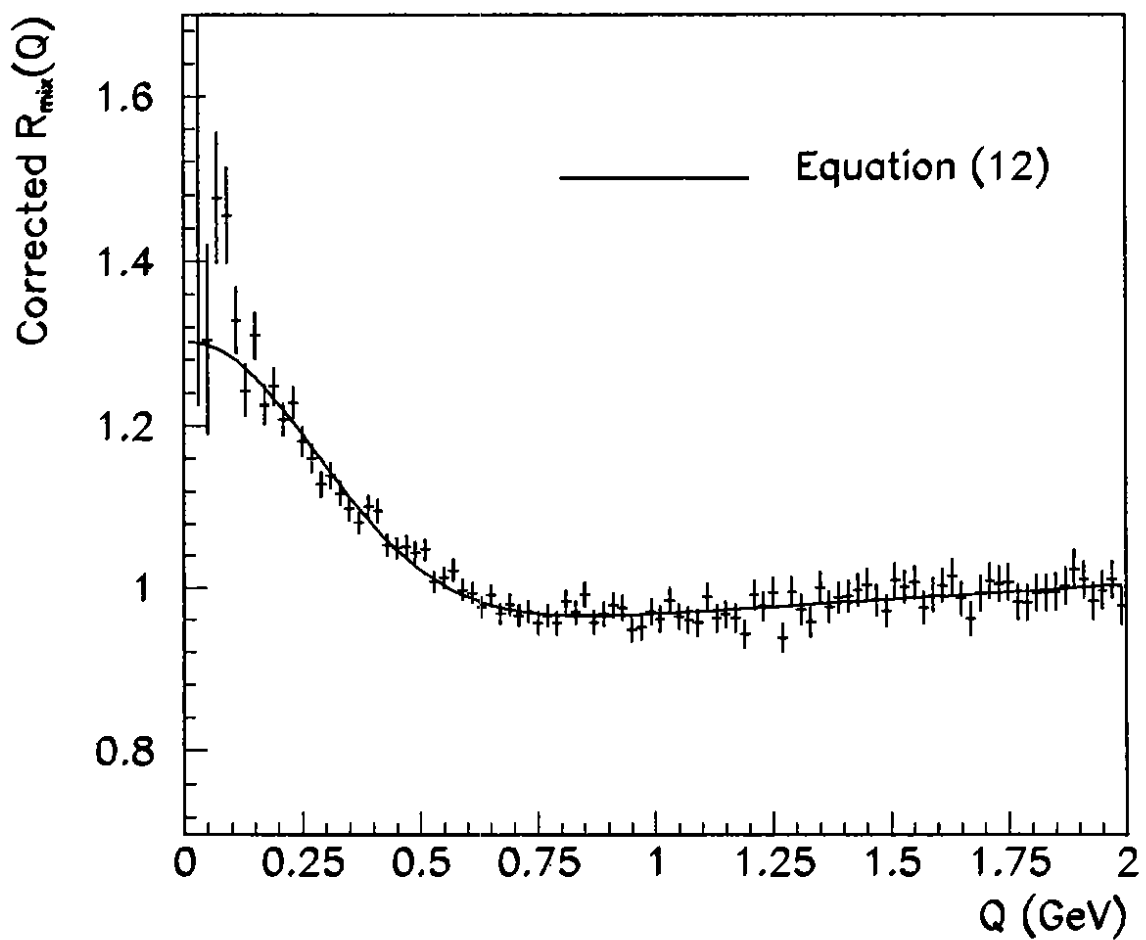


Figure 5b : Corrected $R_{mix}(Q)$

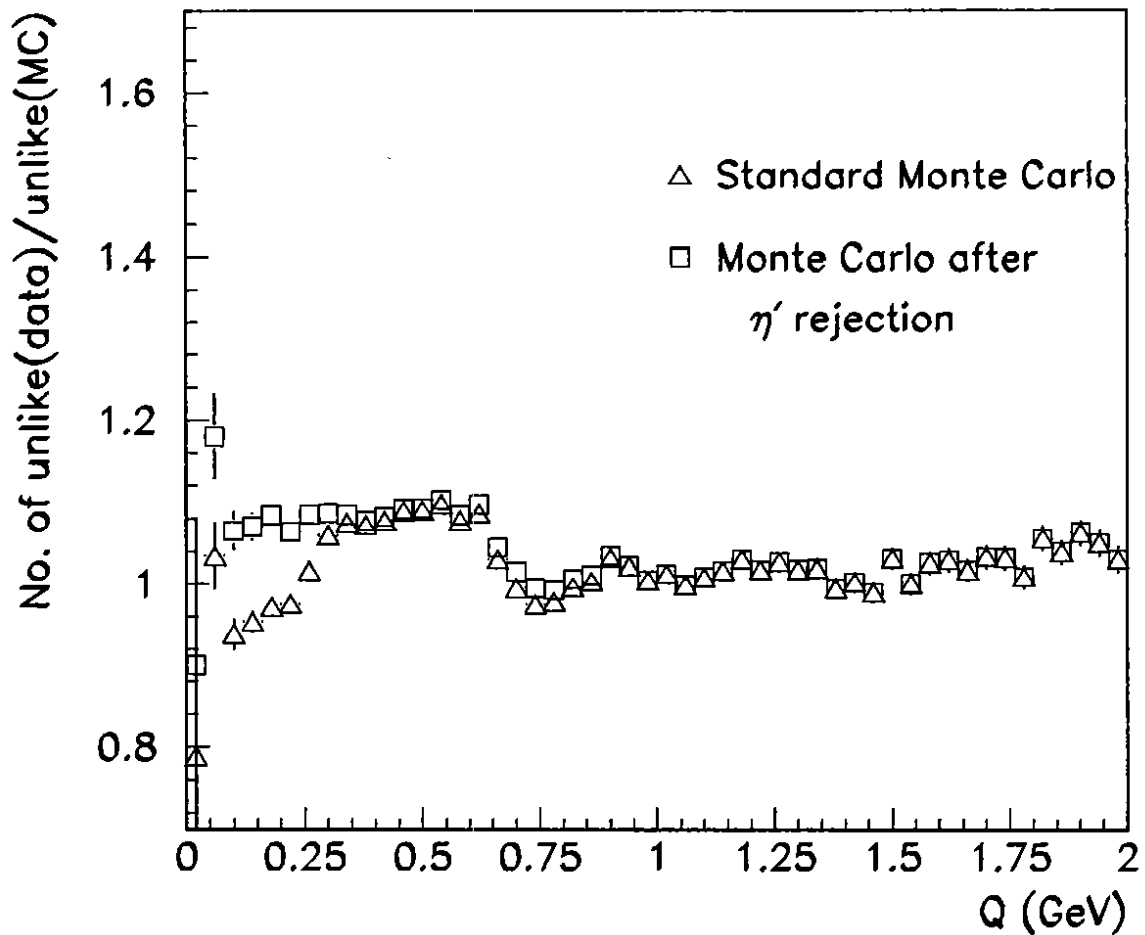


Figure 6a: Comparison of data and MC

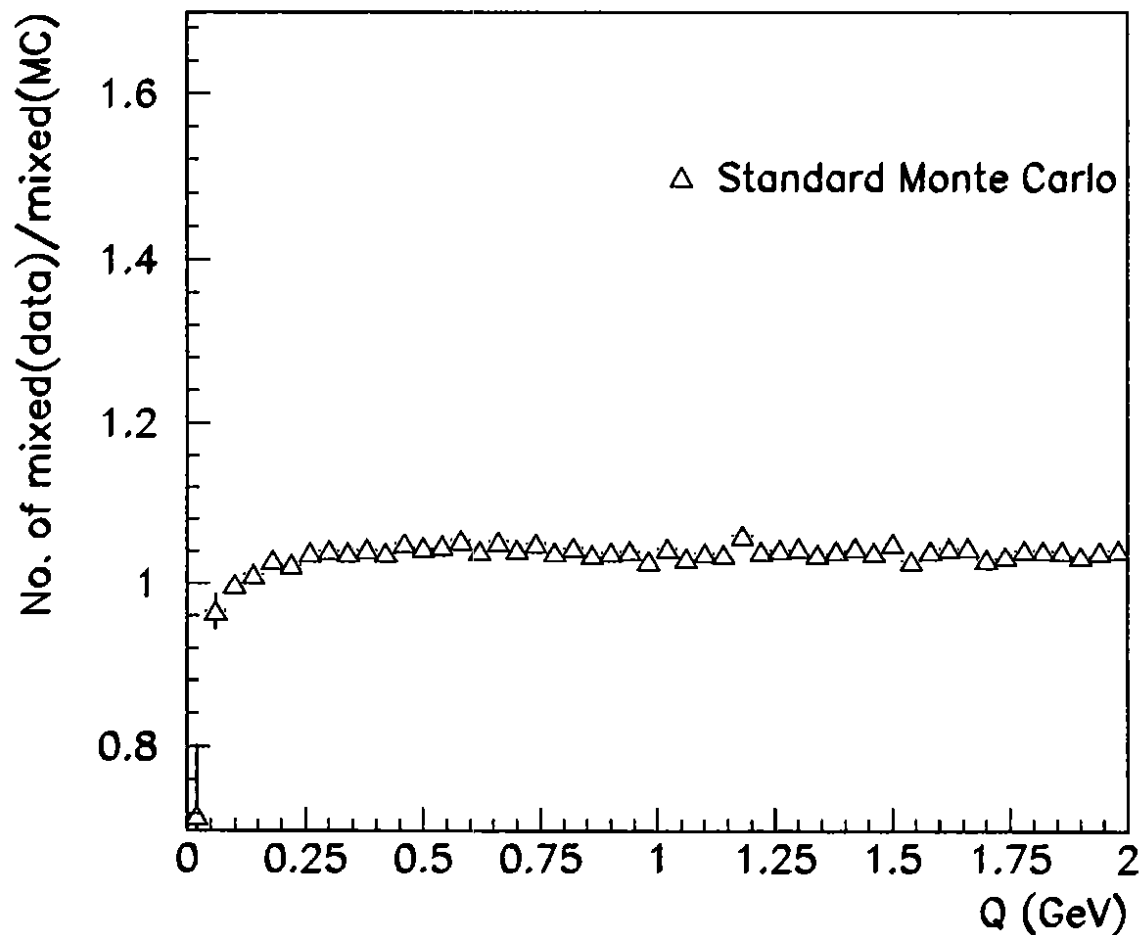


Figure 6b: Comparison of data and MC

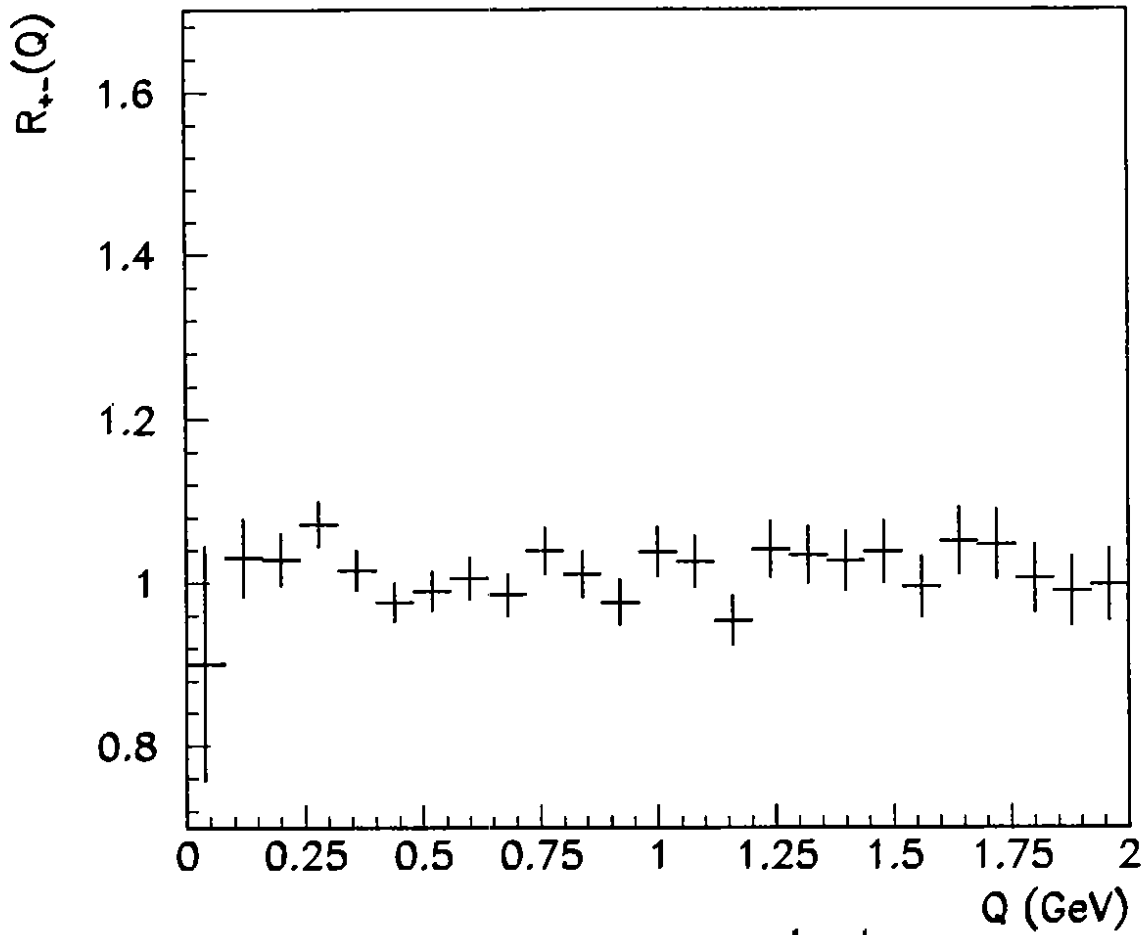


Figure 7: $R_{+-}(Q)$ for $\pi^{\pm}K^{\pm}$ pairs